Biomimetic Catalysis of Catechol Cleavage by O_2 in Organic Solvents − Role of Accessibility of O_2 to Fe^{III} in 2,11-Diaza[3,3](2,6)pyridinophane-Type Catalysts

Nathalie Raffard,[a] Riccardo Carina,[b] A. Jalila Simaan,[a] Joëlle Sainton,[a] Eric Rivière,[a] Luba Tchertanov,[c] Sophie Bourcier,[d] Guy Bouchoux,[d] Michel Delroisse,[b] Frédéric Banse,*[a] and Jean-Jacques Girerd*[a]

Keywords: Enzyme models / Catalysis / Iron / Oxygen / N ligands

Three new complexes, $[Fe(LN_4H_2)Cl_2]^+$, $[Fe(LN_4H_2)(Cat)]^+$, and $[Fe(LN_4H_2)(DBC)]^+$, were synthesized by using the tetradentate macrocyclic ligand LN_4H_2 (where LN_4H_2, Cat, and DBC stand for 2,11-diaza[3,3](2,6) pyridinophane, catecholate, and 3,5-di-*tert*-butylcatecholate, respectively). The structure of $[Fe(LN_4H_2)Cl_2]^+$ was determined by X-ray diffraction. It crystallizes in the monoclinic space group *C*2/*c* with $a = 9.613(1)$, $b = 11.589(1)$, $c = 14.063(2)$ Å, β=110.20(2)°, $V = 1541.9(3)$ Å^3, and $Z = 4$. These complexes were found to catalyze the oxidation of catechol groups using O_2. This was performed in various organic solvents at 20 °C. The reaction rates were measured for the stoichiometric complexes $[Fe(LN_4H_2)(Cat)]^+$ and $[Fe(LN_4H_2)(DBC)]^+$. It was found that despite the relatively high energy of the ligand-to-metal charge transfer O(DBC or Cat)→Fe^{III}, their activity was comparable to that of the fast TPA systems [TPA indicates tris(2-pyridylmethyl)amine]. The oxidation products of $DBCH_2$ have been studied. It has then been shown that the LN_4H_2 systems catalyse by means of both intra- and extradiol cleavage of catechol groups. The existence of multiple reactive pathways can account for the fast reactivity observed.

Introduction

Catechol dioxygenases catalyze the ring cleavage of catechols using O_2 without coreductants. Two sub-classes of these enzymes can be distinguished. Intradiol ones contain a trigonal bipyramidal Fe^{III} ion and catalyze the insertion of both atoms of O_2 between the OH groups [C(1) and C(2)] of the catechol. Two different mechanisms have been proposed to account for their reactivity after the chelation of a doubly deprotonated catecholate. The first one proceeds by electrophilic attack of the catechol by O_2.[1] The alternative pathway implicates the Fe^{II}−semiquinonate character of the Fe^{III}−catecholate moiety generated by the charge transfer from the chelated ring to the metal center. The spin-forbidden rule for a reaction between an organic molecule and dioxygen is bypassed, so the oxidation occurs by the attack of the biradical O_2 on the spin density acquired by the substrate ring.[2] The following steps are the same for both pathways. The O_2 moiety binds to the iron center to yield a peroxo bridge between the metal ion and the substrate. The decomposition of this intermediate then leads to the release of the product and regeneration of the active site. Extradiol catechol dioxygenases contain a square-pyramidal Fe^{II} ion and catalyze the oxidative cleavage of catechols in a different fashion: Both atoms of the dioxygen molecule are inserted between C(1) and C(6) or C(2) and C(3). Que and Ho[2] proposed a mechanism for this subclass of enzymes. The first step of the catalytic cycle involves the chelation of a monoanionic substrate followed by the binding of O_2 to Fe^{II}. The Fe^{III}−superoxo species thus formed is proposed to have nucleophilic character on the distal oxygen atom.[2] The nucleophilic oxygen atom of the superoxo species then attacks the ring at the carbon atoms C(3) or C(6), and the product is released.

Among the models described in the literature,[2,3] the vast majority show intradiol catechol dioxygenase reactivity whereas a few behave as extradiol models.[4−9] Que and coworkers have suggested that the key step for the reactivity of intradiol models resides in the charge transfer from the catecholate to Fe^{III}.[10] Among the known models in the literature, the system based on TPA[11] presents the maximum Fe^{II}−semiquinone character and shows a fast ring cleavage of the catechols in stoichiometric conditions. Koch and Krüger[12] used the LN_4Me_2 macrocyclic ligand to achieve efficient catalysis although the rate was approximately 40 times slower than the stoichiometric TPA system.

Studies of extradiol dioxygenase models are scarce. However, basic requirements such as weak steric hindrance and a vacant coordination site for O_2 on the iron center seem essential.[7,8] An analysis of the structure of $[Fe(LN_4Me_2)cat]^+$ reported by Koch and Krüger[12] revealed that the steric hindrance provided by the methyl groups of the ligand could prevent the formation of the

[a] Laboratoire de Chimie Inorganique, UMR CNRS 8613, Université Paris-Sud,
91405 Orsay, France
[b] Unilever Research, Port Sunlight Laboratory,
Port Sunlight L63 3JW, England
[c] CNRS, Institut de Chimie des Substances Naturelles, UPR 2301,
Avenue de la Terrasse, 91198 Gif/Yvette, France
[d] Laboratoire des Mécanismes Réactionnels, UMR CNRS 7651, Ecole Polytechnique,
91128 Palaiseau, France

  1434−1948/01/0909−2249 $ 17.50+.50/0

peroxo bridge between the Fe^{III} ion and the catecholate. Removing these groups appeared then a matter to favor the formation of the peroxo bridge and speed up the reaction. In the present paper, we investigate the effect of steric hindrance on the reactivity of Fe^{III}–catecholate complexes with O_2. We report the results obtained with the system based on the ligand 2,11-diaza[3,3](2,6) pyridinophane (LN_4H_2) (Scheme 1), the analog of the bulkier LN_4Me_2.

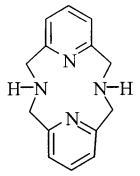

Scheme 1. Schematic representation of the ligand LN_4H_2

Results and Discussion

X-ray Crystal Structure Determination

The starting Fe^{III} complex is $[Fe(LN_4H_2)Cl_2]Cl$. Its structure has been determined. The complex cation is represented in Figure 1. Selected bond lengths and angles are listed in Table 1.

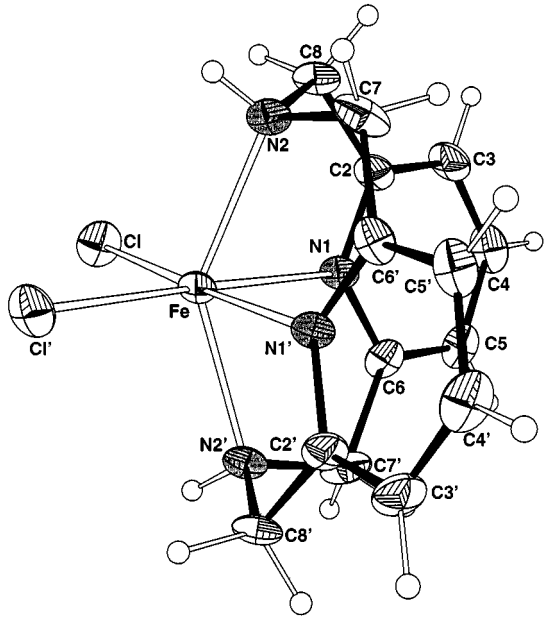

Figure 1. ORTEP plot showing the structure of $[Fe(LN_4H_2)(Cl)_2]^+$ with atom-labeling scheme; primed atoms are related to unprimed ones by symmetry elements of the molecule; displacement ellipsoids are drawn at the 50% probability level; H atoms are shown as small circles of arbitrary radii

It shows an internal C_{2v} symmetry with two mirror planes, one defined by the iron(III) and the *N*-pyridine atoms, and the other by the iron(III) and the *N*-amine atoms. As in previous studies with this macrocycle[13] or its analog LN_4Me_2,[12,14,15] the pseudo-octahedral iron ion is coordinated to the four nitrogen atoms of the ligand leaving two *cis* positions at the metal center that are occupied by two chloro groups in the present species. The ligand is folded along the $N_{amine}-N_{amine}$ axis, the pyridine moieties being nearly perpendicular to each other with a dihedral angle of 96.5(1)°. The $Fe-N_{py}$ distance of 2.09 Å and the $Fe-N_{amine}$ distance of 2.19 Å are slightly shorter than the same distances in the related high-spin $[Fe(LN_4Me_2)Cl_2]^+$ complex.[14] This surprising evolution, especially for the $Fe-N_{amine}$ distances, reflects without ambiguity the decreased steric hindrance at the metal center with LN_4H_2. The Fe–Cl distance of 2.29 Å agrees with the mean value of 2.283(4) Å calculated from other Fe^{III} complexes.[16]

Table 1. Selected bond lengths [Å] and angles [°] for $[Fe(LN_4H_2)(Cl)_2]Cl$; symmetry transformations used to generate equivalent atoms: $-x, y, -z + 1/2$

Fe–N(1)	2.094(1)
Fe–N(2)	2.189(1)
Fe–Cl	2.289(5)
N(1)′–Fe–N(1)	84.95(7)
N(1)–Fe–N(2)	77.51(5)
N(1)–Fe–N(2)′	74.99(5)
N(2)–Fe–N(2)′	142.41(7)
N(1)′–Fe–Cl	175.09(4)
N(1)–Fe–Cl	90.16(4)
N(2)–Fe–Cl	104.39(4)
N(2)′–Fe–Cl	100.83(4)
N(1)–Fe–Cl′	175.09(4)
Cl–Fe–Cl′	94.73(3)

UV/Vis Absorption Spectroscopy

The reaction of the yellow $[Fe(LN_4H_2)Cl_2]Cl$ in MeOH or CH_3CN with a catecholate immediately yielded a deep purple-blue solution. A purple-blue complex can be precipitated on addition of $NaBPh_4$. The UV/Vis spectrum of a solution of the resulting powder or of the solution obtained by mixing $[Fe(LN_4H_2)Cl_2]Cl$ and cat^{2-} shows two intense bands in the visible region. They are assigned as ligand-to-metal charge transfer (LMCT) bands from the doubly deprotonated chelating catecholate to the iron(III) ion.[10,17–19] This charge transfer generates some Fe^{II}–semiquinonate character[10] in the ground state, which is a key factor in the reactivity. The optical data of the catecholate (Cat) or 3,5-di-*tert*-butylcatecholate (DBC) complexes in MeOH or CH_3CN are given in Table 2.

As expected, the DBC species absorbs at a higher wavelength than the Cat species. This observation is consistent with the stronger electron-donating ability of the *tert*-butyl groups leading to an easier charge transfer from the DBC^{2-} to the iron ion.

The LMCT bands of these complexes can be considered as probes for the intradiol reactivity: the lower in energy the LMCT bands are, the faster the intradiol reactivity is. In comparison to other auxiliary ligands[11,20,21] or the close analog LN_4Me_2[12] the LMCT bands of our Fe^{III}–catecholate complexes lie at relatively high energies. However, other factors may be involved in the efficient oxidative cleavage of the catechols, in particular weak bulki-

Table 2. Characteristics of the LMCT bands and second-order rate constants k at 20 °C for $[Fe(LN_4H_2)(Cat)]^+$ and $[Fe(LN_4H_2)(DBC)]^+$, in MeOH and CH_3CN

	$[Fe(LN_4H_2)(Cat)]^+$			$[Fe(LN_4H_2)(DBC)]^+$		
	λ_1 [nm] (ε [$M^{-1}\cdot cm^{-1}$])	λ_2 [nm] (ε [$M^{-1}\cdot cm^{-1}$])	k [$M^{-1}\cdot s^{-1}$]	λ_1 [nm] (ε [$M^{-1}\cdot cm^{-1}$])	λ_2 [nm] (ε [$M^{-1}\cdot cm^{-1}$])	k [$M^{-1}\cdot s^{-1}$]
MeOH	497 (3040)	689 (3230)	0.027	553 (2860)	744 (3070)	8.6
CH_3CN	488 (2960)	704 (3130)	0.45	546 (3050)	753 (3280)	48

ness of the auxiliary ligand[20,22] or spin equilibrium for the iron ion.[23]

Stoichiometric Kinetic Studies

The oxidative cleavage of catechols can be monitored by UV/Vis spectroscopy by following the decay of the LMCT bands with time. This procedure is characteristic of these kinds of studies.[20,21] The complexes $[Fe(LN_4H_2)(Cat)]BPh_4$ and $[Fe(LN_4H_2)(DBC)]BPh_4$ have been dissolved in CH_3CN or MeOH in order to obtain a final concentration in iron about 10 times lower than that of O_2 ($[O_2]$ = 1.62 mM in CH_3CN[24] and $[O_2]$ = 2 mM in MeOH,[25] at 20 °C under air). The kinetic analyses were then carried out by using a pseudo-first-order law. The second-order rate constants, at 20 °C, are tabulated in Table 2. A typical evolution of the LMCT bands during the oxygenation of the catecholate complex and the kinetic analysis are shown in Figure 2.

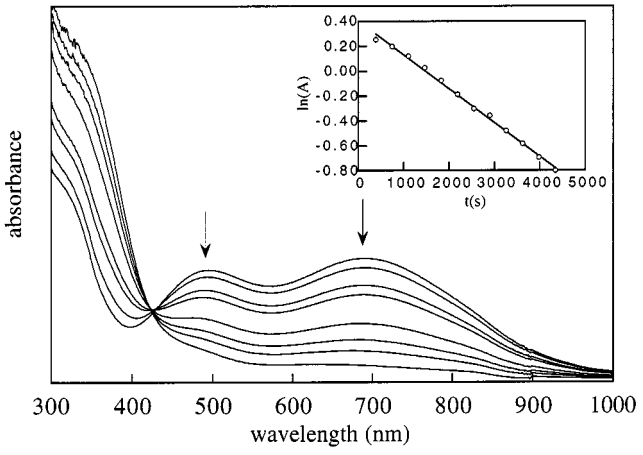

Figure 2. Evolution of the UV/Vis spectrum of $[Fe(LN_4H_2)(Cat)]^+$ in air-saturated MeOH at 20 °C; inset: plot of ln(A) vs. time

Compared to the LN_4Me_2 analog (k = 0.277 10^{-2} $M^{-1}s^{-1}$ for the substrate catecholate, and k = 0.377 $M^{-1}s^{-1}$ for the substrate di-*tert*-butylcatecholate in CH_3CN),[12] one can note a 160-fold increase and a 130-fold increase, respectively. These spectacular accelerations are certainly not attributable to electronic factors as deduced from UV/Vis spectra. Steric factors must be implicated as revealed by the structure analysis of $[Fe(LN_4H_2)Cl_2]^+$. The great accessibility of O_2 to the iron center appears then to be a very important parameter in order to perform a fast ring cleavage of the catechols. The rate constants can also be compared to that of the TPA system, the fastest intradiol catechol dioxygenase model reported so far[11]: in MeOH, the rate constants are very similar to those of TPA (10 vs. 8.6 $M^{-1}s^{-1}$).

Catalytic Catechol Dioxygenase Activity of $[Fe(LN_4H_2)Cl_2]Cl$

In a typical experiment, $[Fe(LN_4H_2)Cl_2]Cl$ was dissolved in CH_3CN, then 50 equiv. of $DBCH_2$ + 2 equiv. of NEt_3 in the same solvent were added. The reaction mixture was analyzed by Electrospray Ionization Mass Spectrometry (ESI-MS) at the end of the reaction, or by ^1H NMR spectroscopy during the course of the reaction, when the sample was prepared in CD_3CN, CD_3OD or $CDCl_3$.

Figure 3. shows the evolution, by NMR spectroscopy, of the reaction mixture in CD_3OD. The results are similar in other solvents. The excess of substrate is sufficient to avoid broadening of the peaks due to the paramagnetism of the Fe^{III} complex. The signals of the free substrate are observed at δ = 1.24, 1.37, 6.72 (d), and 6.73 (d). They disappear during the course of the reaction whereas other signals grow in intensity. The new signals correspond to three major products plus some other minor species that have not been further characterized by this technique. For the major products, the assignments have been made by comparing the spectra with those recorded in CD_3CN or in $CDCl_3$. We also referred to the complete work of Funabiki et al.[4] It appears then that muconic anhydride [the common intradiol cleavage product 3,5-di-*tert*-butyl-1-oxacyclohepta-3,5-diene-2,7-dione (**1**)] is detected at δ = 1.18, 1.27, 6.21 (d), and 6.61 (d). Two extradiol cleavage products are also detected: The first one is 3,5-di-*tert*-butyl-2-pyrone (**2**) (δ = 1.15, 1.24, 6.56, 6.58). The second one is detected at δ = 1.13, 1.16, 5.38, and 6.18. We propose that these signals correspond to the enol form of *cis*,*cis*-3,5-di-*tert*-butyl-2-hydroxymuconic semialdehyde (**3**). Indeed, its keto form has been detected unambiguously in $CDCl_3$ at δ = 1.10, 1.19, 5.28, and 9.75. These values are close to those reported by Funabiki et al.[4] It thus makes sense to propose that the more polar form of this product is stable in the more polar solvent whereas the less polar form is stabilized in the less polar solvent. The by-product 3,5-di-*tert*-butyl-1,2-benzoquinone (**6**) was not detected or only as trace amounts. Due to overlapping of the signals, the final spectrum has been

deconvoluted[26] in order to estimate intradiol versus extradiol cleavage. The results show that the oxygenation of 3,5-di-*tert*-butylcatechol by the LN_4H_2 system proceeds with an intradiol/extradiol ratio close to 1. Attempts to purify the reaction mixture by column chromatography have been unsuccessful due to the instability of the products. As a matter of fact, we cannot report a more quantitative attribution of the products.

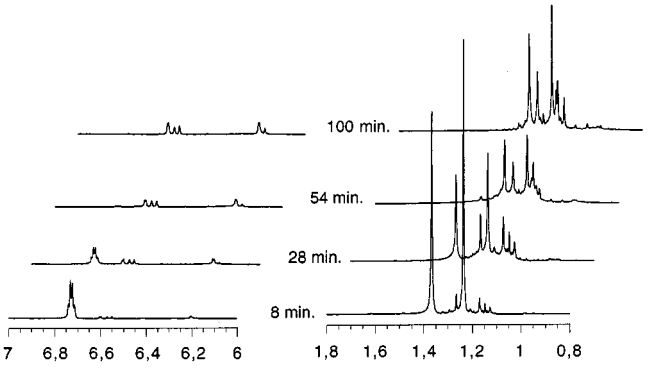

Figure 3. Progress of the reaction of $[Fe(LN_4H_2)(Cl)_2]^+$ + 50 $DBCH_2$ + 2 NEt_3 in air-saturated CD_3OD monitored by ^1H NMR spectroscopy; the peak at δ = 5.38 (see text) is omitted for clarity

The oxygenation products have also been analyzed by ESI-MS from a reaction mixture in CH_3CN. An MeOH/H_2O (0.1% formic acid) mixture has been used for the detection of some species. The 3 major products are observed at *m*/*z* = 237.2 (**1**), *m*/*z* = 209.2 (**2**) and *m*/*z* = 255.4 (**3**). Other peaks are observed; some of them can be assigned as follows: *m*/*z* = 441.6 {4′,6,6′,8-tetrakis(1,1-dimethylethyl)spiro[1,4-benzodioxin-2(3*H*),2′-[2*H*]pyran]-3-one, **4**}, *m*/*z* = 225.3 (3,5-di-*tert*-butyl-5-formyl-2-furanone, **5**) and *m*/*z* = 221.2 (**6**). The results are summarized in Scheme 2.

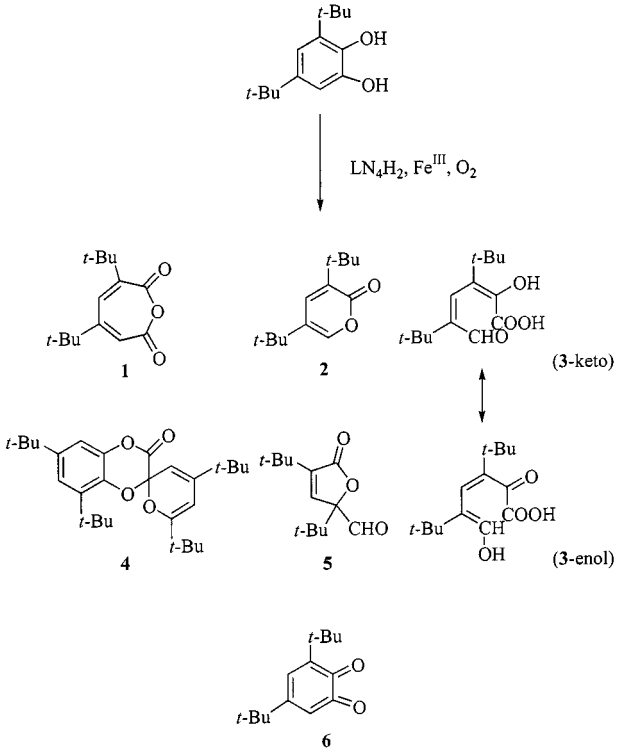

Scheme 2. Oxidation products of 3,5-di-*tert*-butylcatechol detected in this study

To the best of our knowledge, there are only two examples of structurally characterized synthetic iron complexes capable of carrying out extradiol cleavage. They are based on the tridentate ligands TACN (1,4,7-triazacyclononane)[5,7] or hydrotris(3,5-diisopropyl-1-pyrazolyl)-borate[8]. The authors evoke the necessity to dispose of several factors, namely a vacant site around the iron center for the coordination of O_2 and a moderate steric hindrance. Moreover Ito and Que[7] show that Lewis bases such as pyridines must be available in the reaction mixture. They propose that the Lewis base substitutes an oxygen atom of the substrate and thus converts it into a monodentate anion. The structure of the intermediate obtained allows the extradiol cleavage to occur.

Because of the rigidity of the 12-membered LN_4H_2 macrocycle, we never observed species with this ligand acting as tridentate. We therefore report here the first example of extradiol dioxygenase activity with a tetradentate ligand.

As revealed by UV/Vis, $[Fe(LN_4H_2)(DBC)]^+$ has some Fe^{II}–semiquinonate character which is believed to be at the origin of intradiol cleavage activity (pathway 1 in Scheme 3), as usually observed for complexes with tetradentate ligands.[10–12,20,21]

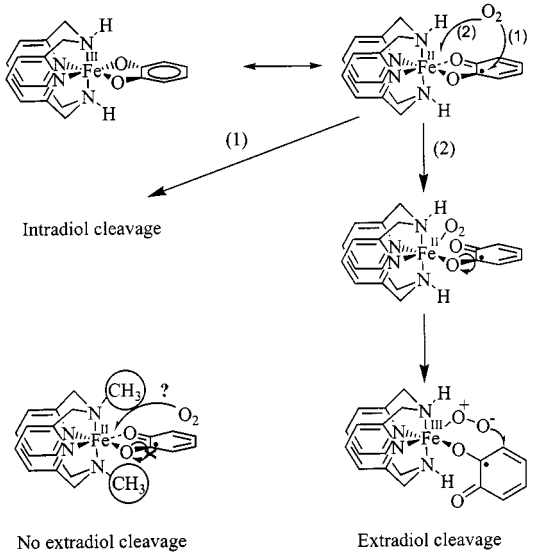

Scheme 3. Proposed mechanism for the reaction of $[Fe(LN_4H_2)(DBC)]^+$ with O_2

For the extradiol cleavage, we propose a mechanism inspired by Ito and Que[7] (see Scheme 3). In one, O_2 binds to the iron center to yield an Fe^{III}–superoxo species leading to the release of an oxygen atom of the enediolate moiety (pathway 2 in Scheme 3). The next sequence is then the ro-

tation of the substrate ring which is permitted due to the weak steric congestion on the amino groups. Finally, the oxygenation proceeds by the attack of the nucleophilic superoxide[2] at the carbon atom adjacent to the C−O group bound to the iron ion yielding extradiol cleavage of the aromatic ring.

The reason why the reactivity pattern of $[Fe(LN_4H_2)(DBC)]^+$ is clearly different from its analog LN_4Me_2 can only be related to the substituents of the macrocycles. The accessibility of the metal center is allowed with LN_4H_2 while the bulkiness of the methyl groups provides a crowded iron center in LN_4Me_2. The Fe^{III}−superoxo species responsible for the extradiol cleavage therefore cannot be obtained with the latter ligand. Moreover, the rotation of the ring catecholate should be forbidden due to the methyl groups. Consequently, the intermediate with the convenient stereospecificity for extradiol cleavage cannot be formed (see Scheme 3). Finally, we propose two reasons, related to the relative steric hindrance of the tetradentate macrocycles, to explain their different reactivity pattern.

The large rate constants observed for our catalyst may thus be due not only to the accessibility to the metal center but also to the existence of multiple reactive paths. To the best of our knowledge, no kinetic data for extradiol cleavage of catechols have been reported. At this stage we therefore cannot conclude whether one hypothesis is more valuable than the other one.

Conclusion

We isolated new Fe^{III} complexes based on the macrocyclic tetradentate ligand LN_4H_2. The structure of the chloro complex $[Fe(LN_4H_2)(Cl)_2]Cl$ has been determined. It reveals that the ligand adopts a bent conformation leaving two *cis* positions at the metal center that are occupied by two chloro ligands. The comparison of its bond lengths with the ones of the related $[Fe(LN_4Me_2)(Cl)_2]^+$ reported by Koch and Krüger bears evidence of the increased accessibility to the metal center in $[Fe(LN_4H_2)(Cl)_2]^+$.

Two other complexes with catecholate groups as exogeneous ligands have been prepared: $[Fe(LN_4H_2)(Cat)]^+$ and $[Fe(LN_4H_2)(DBC)]^+$. Their characterization by optical spectroscopy and ESI-MS are given. The reported complexes react with O_2 and the kinetics of the reaction has been measured. They show one of the fastest catechol dioxygenase reactivity ever reported for coordination compounds.

The catalysis of oxidative cleavage of $DBCH_2$ by $[Fe(LN_4H_2)(Cl)_2]Cl$ has been studied by ^1H NMR and ESI-MS. It indicates that this complex undergoes both intra- and extradiol dioxygenase activity, which is the first case reported with a tetradentate ligand, to date. The fast reactivity observed may thus be due to multiple reactive pathways. A mechanism based on the steric characteristics of the ligand is proposed to explain this tendency.

Experimental Section

General: Starting materials were purchased from Acros and were used as received. Solvents were purchased from Merck and used without purification except when indicated below. Syntheses of catecholate and 3,5-di-*tert*-butylcatecholate complexes were carried out in a glovebox equipped with an O_2/H_2O purifier (Jacomex BS531) − UV/Vis: Varian Cary 5E or Cary 300 Bio equipped with temperature controllers. − MS: VG Quattro II (Micromass, Manchester, UK) triple quadrupole electrospray mass spectrometer. Typical optimized values for the source parameters were: capillary 2.5 kV, counter electrode 0.4 kV, cone voltage 15−50 V, source temperature 80 °C. − NMR spectra were recorded with a Bruker AM250 at 20 °C, using the protonated impurity of the solvent as internal reference.

Synthesis of the Ligand: The ligand LN_4H_2 was prepared according to reported methods[27] and improved with slight modifications.

Syntheses of the Complexes

$[Fe(LN_4H_2)Cl_2]Cl$: A solution of $FeCl_3$ (54.1 mg; 0.33 mmol) in CH_3CN was added dropwise to a solution of LN_4H_2 (80 mg, 0.33 mmol) in CH_2Cl_2. The solution was refluxed for a few minutes and then allowed to cool down. A yellow powder was collected by filtration. Yield 70 mg (50%). Crystals for X-ray analysis were grown from an MeOH solution with aerial diffusion of CH_3CN. − ESI-MS m/z = 366.2 $[Fe(LN_4H_2)Cl_2]^+$. − $[Fe(LN_4H_2)Cl_2]Cl{\cdot}0.8H_2O$ $C_{14}H_{16}N_4Cl_3Fe{\cdot}0.8H_2O$ (416.9): calcd. C 40.33, H 4.25, Cl 25.51, N 13.44; found C 40.75, H 4.05, Cl 24.51, N 13.05.

$[Fe(LN_4H_2)(Cat)]BPh_4$: A solution of catechol (22 mg; 0.2 mmol) and NEt_3 (56 μL; 0.40 mmol) was added dropwise to a dry methanol solution of $[Fe(LN_4H_2)Cl_2]Cl$ prepared in the glovebox at room temperature with 48 mg of LN_4H_2 (0.2 mmol) and 32.4 mg of anhydrous $FeCl_3$ (0.2 mmol). The dark blue solution was stirred for 5 min, then 0.9 equiv. of $NaBPh_4$ (61.4 mg) in dry MeOH was added to give a dark blue microcrystalline powder. The solid was isolated by filtration, washed with MeOH and dried under vacuum. Yield 97 mg (60%). − EI-MS m/z = 404.2 $[Fe(LN_4H_2)(Cat)]^+$. − $[Fe(LN_4H_2)(Cat)]BPh_4{\cdot}1.4CH_3OH$ $C_{44}H_{40}N_4O_2BFe{\cdot}1.4CH_2OH$ (812.8): calcd. C 70.97, H 5.98, B 1.41, Fe 7.27, N 7.29; found C 70.90, H 5.53, B 1.33, Fe 7.1, N 7.43.

$[Fe(LN_4H_2)(DBC)]BPh_4$: The experimental procedure was similar to the one described for $[Fe(LN_4H_2)(Cat)]BPh_4$. Yield 120 mg (70%). − EI-MS m/z = 516.4 $[Fe(LN_4H_2)(DBC)]^+$. − $[Fe(LN_4H_2)(DBC)]BPh_4{\cdot}1.1CH_3OH$ $C_{52}H_{56}N_4O_2BFe{\cdot}1.1CH_3OH$ (869.4): calcd. C 73.23, H 6.99, B 1.24, Fe 6.41, N 6.43; found C 73.20, H 7.01, B 1.27, Fe 6.45, N 6.67.

Structure Determination: The crystal data of $[Fe(LN_4H_2)Cl_2]Cl$ and the parameters of data collection are summarized in Table 3. A flattened octahedron-shaped yellow crystal with the dimensions 0.65 × 0.40 × 0.30 mm of $[Fe(LN_4H_2)Cl_2]Cl$ was chosen for the X-ray diffraction experiment. The unit-cell and intensity data were measured with an Enraf−Nonius CAD-4 diffractometer with graphite-monochromated Mo-K_α radiation (λ = 0.71070 Å). The cell constants were obtained by least-squares procedures based upon the 2Θ values of 25 reflections measured in the ranges $18.3° < 2\Theta < 25.2°$ at ambient temperature. During data collection three control reflections were measured every 3 h; the crystal was stable, and the check reflections showed a slight decay in intensity of only 7% during the X-ray data collection. A total of 2335 reflections were collected in the range $5.6° < 2\Theta < 59.9°$

within [$-13 \le h \le 13$, $0 \le k \le 16$, $0 \le l \le 19$]. From 2249 independent reflections, 2186 were considered as observed [$I > 2\sigma(I)$]. The structure was solved by direct methods with the program Shelxs86[28] and refined by using the Shelxl93 program.[29] The drawing was prepared with OrtepII.[30] The molecular cation was located in a special crystallographic position with the iron atom at the twofold rotation axis, along with the chloride anion. The structure was refined anisotropically (non-hydrogen atoms) by full-matrix least-squares approximation based on F^2. The hydrogen atom at the secondary nitrogen atom was localized in a difference Fourier synthesis and refined isotropically. Other hydrogen atom positions were calculated by assuming geometrical positions and were included in the structural model. Final weighting scheme was $w = 1/[\sigma^2(F_o^2) + (0.0411P)^2 + 2.0320P]$, where $P = (F_o^2 + 2F_c^2)/3$. The final refinement of this model was continued until convergence when $R1 = 0.0302$ for $F^2 > 2\sigma(F^2)$ and $R_w = 0.0806$ were reached. The final difference map showed the largest residual peaks which are 0.424 and -0.641 e·Å^{-3}. The two largest peaks were found at the Fe and Cl atoms. Complete crystallographic data (excluding structure factors) for the structure reported in this paper has been deposited at the Cambridge Crystallographic Data Centre with no. CCDC-148680. Copies of the data can be obtained free of charge on application to CCDC, 12 Union Road, Cambridge CB2 1EZ, UK [Fax: (internat.) + 44-1223/336-033, E-mail: deposit@ccdc.cam.ac.uk, World Wide Web: http://www.ccdc.cam.ac.uk].

Table 3. Crystal data and structure refinement for $[Fe(LN_4H_2)(Cl)_2]Cl$

Empirical formula	$C_{14}H_{16}Cl_3Fe_1N_4$
Molecular mass	402.51
Temperature	294(2) K
Wavelength (Mo-K_α)	0.71070 Å
Crystal system	monoclinic
Space group	*C*2/*c*
a [Å]	9.613(1)
b [Å]	11.589(1)
c [Å]	14.063(2)
β [°]	110.20(2)
Volume [Å^3]	1541.9(3)
Z	4
d_x [Mg/m^3]	1.728
μ [mm^{-1}]	1.498
F(000)	820
Crystal size [mm]	0.65 × 0.40 × 0.30
Θ range [°]	2.78−29.95
Index ranges	$-13 \le h \le 13$
	$0 \le k \le 16$
	$0 \le l \le 19$
$N_{collect}$	2335
N_{indt}	2249 [*R*(int) = 0.0398]
N_{obs}	2186 [$I > 2\sigma(I)$]
$R1$ [$I > 2\sigma(I)$]	0.0302
$wR2$	0.0806
ρ_{max} [eÅ^{-3}]	0.424
ρ_{min} [eÅ^{-3}]	−0.641

[1] J. D. Lipscomb, A. M. Orville, *Met. Ions Biol. Syst.* **1992**, *28*, 285.
[2] L. Que, R. Y. N. Ho, *Chem. Rev.* **1996**, *96*, 2607.
[3] T. Funabiki, *Catalysis by Metal Complexes*, Kluwer Academic Publishers, Dordrecht/Boston/London, **1997**, p. 19.
[4] T. Funabiki, A. Mizoguchi, T. Sugimoto, S. Tada, M. Tsudi, H. Sakamoto, S. Yoshida, *J. Am. Chem. Soc.* **1986**, *108*, 2921.
[5] A. Dei, D. Gatteschi, L. Pardi, *Inorg. Chem.* **1993**, *32*, 1389.
[6] T. Funabiki, I. Yoneda, M. Ishikawa, M. Ujiie, Y. Nagai, S. Yoshida, *Chem. Commun.* **1994**, 1453.
[7] M. Ito, L. Que, *Angew. Chem. Int. Ed. Engl.* **1997**, *36*, 1342.
[8] T. Ogihara, S. Hikichi, M. Akita, Y. Moro-oka, *Inorg. Chem.* **1998**, *37*, 2614.
[9] H. Weiner, R. G. Finke, *J. Am. Chem. Soc.* **1999**, *121*, 9831.
[10] D. D. Cox, L. Que, *J. Am. Chem. Soc.* **1988**, *110*, 8085.
[11] H. G. Jang, D. D. Cox, L. Que, *J. Am. Chem. Soc.* **1991**, *113*, 9200.
[12] W. O. Koch, H. J. Krüger, *Angew. Chem. Int. Ed. Engl.* **1995**, *34*, 2671.
[13] R. Carina et al., unpublished results.
[14] W. O. Koch, V. Schünemann, M. Gerdan, A. X. Trautwein, H. J. Krüger, *Chem. Eur. J.* **1998**, *4*, 686.
[15] W. O. Koch, V. Schünemann, M. Gerdan, A. X. Trautwein, H. J. Krüger, *Chem. Eur. J.* **1998**, *4*, 1255.
[16] F. H. Allen, O. Kennard, *Chem. Design Aut. News* **1993**, *8*, 31.
[17] D. D. Cox, S. J. Benkovich, L. M. Bloom, F. C. Bradley, M. J. Nelson, L. Que, D. E. Wallick, *J. Am. Chem. Soc.* **1988**, *110*, 8085.
[18] S. Salama, J. D. Stong, J. B. Neilands, T. G. Spiro, *Biochemistry* **1978**, *17*, 3781.
[19] A. Dei, D. Gatteschi, L. Pardi, *Inorg. Chem.* **1993**, *32*, 1389.
[20] P. Mialane, L. Tchertanov, F. Banse, J. Sainton, J.-J. Girerd, *Inorg. Chem.* **2000**, *39*, 2440.
[21] M. Pascaly, M. Duda, A. Rompel, B. H. Sift, W. Meyer-Klaucke, B. Krebs, *Inorg. Chim. Acta* **1999**, *291*, 289.
[22] M. Pascaly, C. Nazikkol, F. Schweppe, A. Wiedemann, K. Zurlinden, B. Krebs, *Z. Anorg. Allg. Chem.* **2000**, *626*, 50.
[23] A. J. Simaan, M.-L. Boillot, E. Rivière, A. Boussac, J.-J. Girerd, *Angew. Chem. Int. Ed.* **2000**, *39*, 196.
[24] Value obtained by dividing by 5 the concentration under pure O_2 (8.1 mM, see for example ref.[12]).
[25] J. Tokunaga, *J. Chem. Eng. Data* **1975**, *20*, 41.
[26] The final spectrum has been deconvoluted with a sub-program of WinNMR 5.1 software, Bruker. Only the peaks attributed to the three major products have been analyzed in downfield and upfield regions. The results obtained in both regions have been compared. We made the hypothesis that the minor products were negligible.
[27] [27a]B. Alpha, E. Anklam, R. Deschenaux, J.-M. Lehn, M. Pietrakiewicz, *Helv. Chim. Acta* **1988**, *71*, 1042. − [27b] F. Bottino, M. Di Grazia, P. Finocchiaro, F. R. Fronczek, A. Mamo, S. Pappalardo, *J. Org. Chem.* **1988**, *53*, 3521.
[28] G. M.Sheldrick, *Shelxs86*, Univ. of Göttigen, Germany, **1986**.
[29] G. M. Sheldrick, *Shelxl93*, Univ. of Göttigen, Germany, **1993**.
[30] C. K. Johnson, *OrtepII*, Report ORNL-5138. Oak Ridge National Laboratory, Tennessee, USA, **1976**.

Received February 16, 2001
[I01054]